REPORT OF INVESTIGATIONS/1994

A Technique for Measuring the Dielectric Properties of Minerals at Microwave Heating Frequencies Using an Open-Ended Coaxial Line

By J. B. Salsman and S. P. Holderfield

UNITED STATES DEPARTMENT OF THE INTERIOR

BUREAU OF MINES

U.S. Department of the Interior
Mission Statement

As the Nation's principal conservation agency, the Department of the Interior has responsibility for most of our nationally-owned public lands and natural resources. This includes fostering sound use of our land and water resources; protecting our fish, wildlife, and biological diversity; preserving the environmental and cultural values of our national parks and historical places; and providing for the enjoyment of life through outdoor recreation. The Department assesses our energy and mineral resources and works to ensure that their development is in the best interests of all our people by encouraging stewardship and citizen participation in their care. The Department also has a major responsibility for American Indian reservation communities and for people who live in island territories under U.S. administration.

Report of Investigations 9519

A Technique for Measuring the Dielectric Properties of Minerals at Microwave Heating Frequencies Using an Open-Ended Coaxial Line

By J. B. Salsman and S. P. Holderfield

UNITED STATES DEPARTMENT OF THE INTERIOR
Bruce Babbitt, Secretary

BUREAU OF MINES

This report is based on work done under an agreement between the University of Alabama and the U.S. Bureau of Mines.

International Standard Serial Number
ISSN 1066-5552

CONTENTS

ILLUSTRATIONS

TABLE

UNIT OF MEASURE ABBREVIATIONS USED IN THIS REPORT

cm	centimeter	mm	millimeter
GHz	gigahertz	pct	percent
g	gram	μm	micrometer
g/cm³	gram per cubic centimeter	Ω	ohm
kHz	kilohertz	°C	degree Celsius
MHz	megahertz		

A TECHNIQUE FOR MEASURING THE DIELECTRIC PROPERTIES OF MINERALS AT MICROWAVE HEATING FREQUENCIES USING AN OPEN-ENDED COAXIAL LINE

By J. B. Salsman[1] and S. P. Holderfield[2]

ABSTRACT

As part of the research effort on investigating the effects of microwave energy on the chemical and physical properties of minerals and ores, the U.S. Bureau of Mines (USBM) Tuscaloosa Research Center has conducted research to measure the dielectric properties of these materials. The objective was to establish a reliable database for use in predicting the effects of microwave heating on a wide range of minerals.

The dielectric constants and loss factors of minerals, commonly referred to as the dielectric properties, were determined utilizing the theory of microwave propagation through an open-ended, air-filled coaxial line that was terminated at its open end with the particular mineral under investigation.

In this phase of microwave research, the USBM measured the dielectric properties of powdered minerals with medium to high electrical conductivities in the frequency range of 300 MHz to 3 GHz and as a function of temperature from 25 to 325 °C. Since the minerals were prepared as powders, techniques were used to relate the measured dielectric properties of the powdered minerals to the dielectric properties of the mineral at its theoretical or natural density.

[1]Electrical engineer, Tuscaloosa Research Center, U.S. Bureau of Mines, Tuscaloosa, AL (now with Salt Lake City Research Center, U.S. Bureau of Mines, Salt Lake City, UT).

[2]Chemical engineer, Tuscaloosa Research Center.

INTRODUCTION

Major research efforts are underway worldwide on the use of microwave energy in various processing techniques. Deterrents to these research efforts are the lack of sufficient data on the electrical properties of materials (including minerals), and the lack of personnel trained in microwave heating technology. It is very likely that microwave energy may offer many advantages to minerals beneficiation and processing techniques; however, it is difficult to exploit these advantages without an understanding of the electrical properties of minerals. As part of its mission to advance research in processing techniques, the U.S. Bureau of Mines (USBM) is studying the use of microwave energy.

The electrical properties of a mineral are those properties that characterize how that mineral is affected by an electric field, and these properties may, and often do, change with frequency. The electrical properties of minerals are also temperature dependent. At the microwave heating frequencies of 300 MHz to 3 GHz these properties are referred to as the dielectric properties of minerals, namely the dielectric constant and the loss tangent. The dielectric constant determines how much energy can be stored in a material, while the loss tangent is proportional to the amount of energy that is converted to heat. The product of these two terms, the loss factor, determines how well a material will absorb microwave energy.

Currently, a hiatus exists in the literature on the dielectric properties of minerals at microwave heating frequencies (*1-4*).[3] One important reason for this lack of data is that until the recent development of advanced electronic equipment such as the network analyzer, it was very difficult to develop successful measuring systems in this frequency range. This range is too high for radio-frequency techniques and is at the low-frequency end of the microwave spectrum. However, it is this frequency range that is of interest, for it includes the frequencies allocated by the Federal Communications Commission for use in industrial, scientific, medical, and domestic applications (915 MHz, 2.45 GHz, and 22 GHz); the widely used microwave heating frequencies are 915 MHz and 2.45 GHz.

Microwave technology is beginning to find many successful uses in industrial applications other than food preparation or communications. Recent investigations of the use of microwave energy as a heat source in materials-processing techniques have shown several advantages over conventional methods of heating. For example, studies conducted on microwave processing of ceramics and composite materials have shown improved microstructural properties in the final product along with a reduction in energy requirements and processing times (*5-7*). But research is limited in this area because the dielectric properties of minerals and most materials at microwave heating frequencies are virtually unknown. In order to predict whether microwave energy may be a viable tool for use in the minerals industry, these properties must be known, otherwise trial and error methods are the only alternative.

MEASUREMENT OF THE DIELECTRIC PROPERTIES OF MINERALS

The USBM Tuscaloosa Research Center has developed several methods for measuring the dielectric properties of materials at microwave heating frequencies. The method described in this report involves placing the material under investigation at the end of an open-ended coaxial line and measuring the reflection coefficient at the material and coaxial line interface. A network analyzer can be very instrumental in performing this type of reflection-coefficient measurements. This method is very versatile since measurements can be performed at microwave heating frequencies, and it is capable of measuring liquids, solids, and powders. This method is also capable of measuring the dielectric properties of minerals as a function of temperature and density, which significantly adds to the overall effectiveness of the measurement system. However, measurements of the dielectric properties of materials having small losses can not be performed accurately using a one port, open-ended coaxial method because of the fringing fields associated with this type of system. This system can measure the value of the dielectric constant quite accurately for low-loss materials, but the value of the loss factor becomes random.

THEORY OF MEASUREMENT

The method of measuring the dielectric constant, ε_r', and loss factor, ε_r'', involves placing the mineral sample, shown as a load in figure 1, at the end of an open-ended coaxial line and measuring the complex reflection coefficient, Γ^*, at the end of the line. From Γ^*, the dielectric properties can be determined.

[3]Italic numbers in parentheses refer to items in the list of references preceding the appendix.

Figure 1

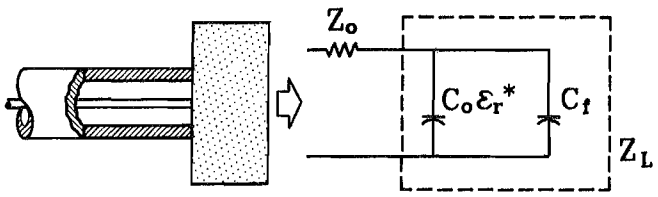

Equivalent circuit of a sample at the end of a coaxial line.

The complex reflection coefficient, Γ^*, can be expressed in terms of the characteristic impedance of a coaxial line, Z_o, and a load impedance, Z_L, as follows (*8*):

$$\Gamma^* = \frac{Z_L - Z_o}{Z_L + Z_o}. \qquad (1)$$

From the model of figure 1, the load impedance is represented as two capacitors in parallel, one of which is written in terms of the complex dielectric constant. Basic circuit analysis shows that the equivalent load impedance can then be expressed as (*9*)

$$Z_L = \frac{1}{j\omega(C_o\varepsilon_r^* + C_f)}, \qquad (2)$$

where ω = the angular frequency, $2\pi f$,

f = measurement frequency,

C_o and C_f = fringing capacitances associated with the coaxial line,

$j = \sqrt{-1}$,

and ε_r^* = complex dielectric constant of the material at the end of the line.

Substituting the value of the load impedance of equation 2 into equation 1 yields an expression for the complex reflection coefficient in terms of the complex dielectric constant, ε_r^*,

$$\Gamma^* = \frac{1 - j\omega Z_o(C_o\varepsilon_r^* + C_f)}{1 + j\omega Z_o(C_o\varepsilon_r^* + C_f)}. \qquad (3)$$

Rearranging equation 3 and solving for the complex dielectric constant yields

$$\varepsilon_r^* = \frac{1 - \Gamma^*}{j\omega Z_o C_o(1 + \Gamma^*)} - \frac{C_f}{C_o}. \qquad (4)$$

However, it is necessary to extract from ε_r^* the values of ε_r', the dielectric constant, and ε_r'', the loss factor. This can be accomplished by expressing ε_r^* with real and imaginary parts,

$$\varepsilon_r^* = \varepsilon_r' - j\varepsilon_r''. \qquad (5)$$

Similarly, the complex reflection coefficient can be written as

$$\Gamma^* = \Gamma\cos\varphi + j\Gamma\sin\varphi, \qquad (6)$$

where Γ = magnitude of the complex reflection coefficient,

and φ = phase.

By substituting for the complex terms of ε_r^* and Γ^* in equation 4 and separating it into its real and imaginary parts, two expressions are obtained, one in terms of ε_r', and the other in terms of ε_r''.

$$\varepsilon_r' = \frac{-2\Gamma\sin\varphi}{\omega Z_o C_o(1 + 2\Gamma\cos\varphi + \Gamma^2)} - \frac{C_f}{C_o}, \qquad (7)$$

and

$$\varepsilon_r'' = \frac{1 - \Gamma^2}{\omega Z_o C_o(1 + 2\Gamma\cos\varphi + \Gamma^2)}. \qquad (8)$$

From equations 7 and 8, the loss tangent, $\tan\delta$, can be calculated as follows:

$$\tan\delta = \frac{\varepsilon_r''}{\varepsilon_r'}. \qquad (9)$$

Since Z_o is the constant characteristic impedance of the line and the values of Γ and φ are measured, one only needs to determine the values of C_o and C_f, the fringing capacitances of the line, to determine the dielectric constant, loss factor, and thus the loss tangent of the material at the end of the open-ended coaxial line.

DETERMINATION OF C_o AND C_f

The determination of C_o and C_f can become quite cumbersome; however, it is crucial to the measurement technique (*10*). The first step is to solve equations 7 and 8 in terms of the capacitances, C_o and C_f.

$$C_o = \frac{1 - \Gamma^2}{\omega Z_o \varepsilon_r''(1 + 2\Gamma\cos\varphi + \Gamma^2)}, \qquad (10)$$

and

$$C_f = \frac{-2\Gamma\sin\varphi}{\omega Z_o \varepsilon_r''(1 + 2\Gamma\cos\varphi + \Gamma^2)} - \varepsilon_r' C_o. \qquad (11)$$

From equations 10 and 11, C_o and C_f can be determined through an iterative process. The procedure is to place materials of known dielectric properties at the end of the open-ended coaxial line and measure the magnitude and phase of the reflection coefficient at the end of the line.

For a first approximation, assume C_f equal to zero. Using equation 10 and measuring the reflection coefficient of a material with sufficiently high dielectric properties, calculate a value for C_o. Using this value of C_o, place a material with low dielectric properties at the end of the coaxial line and measure the reflection coefficient. (Using a low-loss material to calculate the values of C_o and C_f may seem to contradict the limitations given earlier; however, only the ε_r' term is used in this procedure.) From equation 11, calculate a value of C_f. Using equation 11, again, and this new value of C_f, calculate a new value of C_o with measured reflection-coefficient data from a material with high dielectric properties. This new C_o is C_{o1}. In order to judge whether these values of capacitances are suitable values of C_o and C_f, compare C_o and C_{o1}. If they are not equal, the process must be repeated a number of times using the last calculated values of C_o or C_{o1}, and C_f until the values of the capacitances converge. It should be noted that a value of C_o and C_f must be determined for each measurement frequency since these quantities are frequency dependent.

One must be careful when evaluating the values of the fringing capacitances, for these can determine the success or failure of the measurement system. This is especially true when working at frequencies greater than 1 GHz. At the higher frequencies, a new term must be added into the equivalent circuit of figure 1 where the capacitance, $C_o\varepsilon_r^*$, must be determined as $(C_o + Af^2)\varepsilon_r^*$; f is the frequency, and A is a constant dependent on the dimensions of the coaxial line and the dielectric properties of the material at the end of the line. As the frequency increases the wavelength decreases, and the assumption, $\lambda\varepsilon_r' >> (b-a)$, (where b is the radius of the outer conductor of the coaxial line and a is the radius of the inner conductor, see figure 2) is no longer valid, especially for high-loss materials and $_r = \lambda/\sqrt{\varepsilon_r'}$. At this point, the A term given above becomes significant. For the purposes discussed in this report, evaluation of the new capacitance term became necessary at frequencies above 1 GHz and was determined quite similarly to that described above; however, the iterations became somewhat more involved.

SELECTION OF REFERENCE MATERIALS FOR DETERMINING CAPACITANCES

The high-loss materials chosen to determine the fringing capacitance were saline solutions, since their dielectric properties could be calculated as a function of temperature, normality (N), and frequency (*11*). Two of the low-loss materials used were cyclohexane, and 1,2-dichloroethane, which were obtained from the National Institute of Standards and Technology. Other low-loss reference materials used were air, trichloroethylene, and

Figure 2

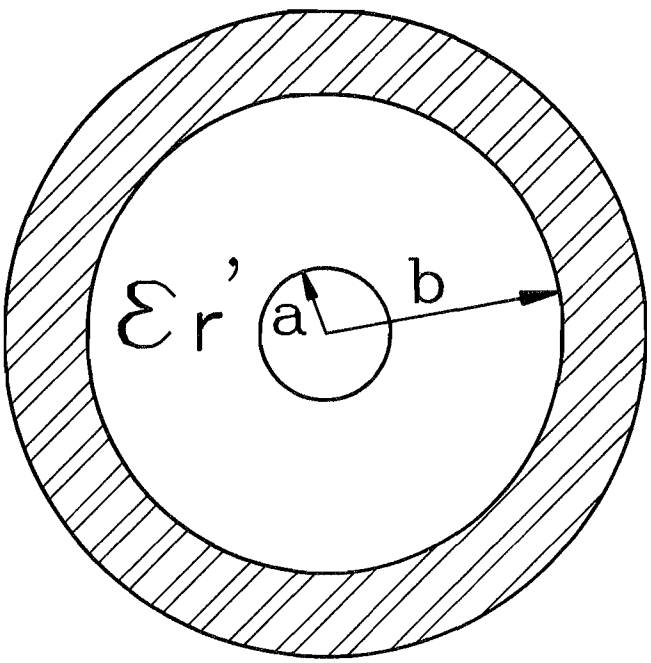

Cross section of a typical coaxial line.

Teflon polytetrafluoroethylene. The dielectric properties of the trichloroethylene and Teflon polytetrafluoroethylene were measured previously by a technique developed by the USBM and compared favorably to referenced data (*12*). Saline solutions of normalities other than those used to determine the values of the fringing capacitances were used to evaluate the accuracy of the measurement procedure. Table 1 gives the results of 0.2-N saline solution measured by this technique given the values of C_o and C_t calculated from 0.1-, 0.5-, and 0.7-N saline solutions along with Teflon polytetrafluorethylene, dichloroethane, and cyclohexane.

DETERMINATION OF DENSITY EFFECTS

Natural minerals come in varied shapes and sizes. Most minerals are not found in nature as large solid specimens, but as tiny fragments mixed with other minerals that have to be separated in order to acquire a pure sample for dielectric property measurements. In the process of separating the minerals for this study, the samples had to be reduced to a powder-like substance. However, the measured dielectric properties of this powdered mineral did not represent those properties of that mineral found in its natural state, thus methods needed to be explored for determining the dielectric properties of a material based on the given data for the natural or particle density of the powdered sample.

The U.S. Department of Agriculture (USDA) has been conducting research on evaluating the dielectric properties of various materials for several years. During these studies, the need arose to determine dielectric properties as a function of density and relate this information to those properties at a different density (*13*). After considerable evaluation, the USBM used this technique and incorporated the method into its measurement system.

Table 1.—Comparison of dielectric constant and loss factor of measured and calculated data for a 0.2-N saline solution

Frequency, MHz	Dielectric constant, ε_r'			Loss factor, ε_r''		
	Measured value	Known value	Difference, pct	Measured value	Known value	Difference, pct
36.07	71.50	75.86	5.72	928.29	914.73	1.48
45.41	73.49	75.86	3.12	736.57	726.66	1.36
57.16	74.35	75.86	1.99	584.69	577.30	1.28
71.97	75.14	75.86	0.95	464.34	458.67	1.24
90.60	75.46	75.85	0.51	368.88	364.47	1.21
114.05	75.58	75.85	0.36	293.07	289.68	1.17
143.59	75.64	75.85	0.28	233.00	230.31	1.17
180.77	75.74	75.85	0.15	185.33	183.21	1.16
227.57	75.78	75.84	0.08	147.62	145.86	1.21
286.50	75.78	75.84	0.08	117.74	116.29	1.25
360.68	75.81	75.83	0.03	94.14	92.90	1.33
454.07	75.75	75.81	0.08	75.55	74.46	1.46
571.64	75.79	75.78	0.01	60.81	59.99	1.37
719.65	75.66	75.74	0.11	49.45	48.71	1.52
905.98	75.55	75.67	0.16	40.65	40.02	1.57
1,089.23	75.41	75.59	0.24	35.19	34.63	1.62
1,309.55	75.24	75.47	0.30	31.08	30.40	2.24
1,648.62	74.83	75.25	0.56	27.04	26.55	1.85
2,075.49	74.85	74.90	1.40	23.85	24.09	1.00
2,612.89	74.81	74.35	0.62	22.37	22.86	2.14
3,000.00	74.43	73.88	0.74	22.74	22.67	0.31

MATHEMATICAL RELATIONSHIPS

The quadratic dependence of ε_r' and ε_r'' on density was expressed by Kent (*14*) as

$$\varepsilon_r' = c\rho^2 + d\rho + 1, \quad (12)$$

and

$$\varepsilon_r'' = k\rho^2 + \ell\rho + 0, \quad (13)$$

where ρ = density of the air-powder mixture,

ε_r' = 1 at zero density,

and ε_r'' = 0 at zero density.

(c, d, k, and ℓ are constants for a given material at a given frequency.)

Also, work at the USDA showed that the linearity of ε_r' with the density of a powdered material can be expressed as

$$\sqrt{\varepsilon_r'} = m\rho + 1, \quad (14)$$

where m = slope of the line,

and ρ = density of the air-powder mixture.

The dielectric constant for air (ρ = 0) is unity for the mixture.

It becomes obvious that when squaring equation 14, equations 14 and 12 become equivalent, where $c = m^2$ and $d = 2m$. Thus, if this relationship holds, measurement of the dielectric constant of a powdered sample at a given density, along with the $\rho = 0$ and $\varepsilon_r' = 1$ intercept, provides enough information for the dielectric constant to be determined at any density including that of a solid material.

A linear relationship between a function of the loss factor and density can also be obtained by completing the square of equation 13. The result is given by

$$\sqrt{\varepsilon_r'' + e} = \rho\sqrt{\ell} + \sqrt{e}, \quad (15)$$

where $e = \ell^2/4k$.

However, a single measurement will not suffice for the evaluation of ε_r'' since the constant e also must be determined. Two measurements will be sufficient for the determination of the loss factor; although, as more measurements are taken as a function of density, the evaluation of the slope term for both the dielectric constant and loss factor becomes more precise.

EQUIPMENT

The measurement system consists of an open-ended coaxial line that is connected to a computer-controlled network analyzer and a mineral sample placed at the opposite end of the coaxial cable. The reflection coefficient at the end of the coaxial cable is measured by the network analyzer in the frequency range of 300 MHz to 3 GHz, and the dielectric constant and loss factor of the mineral can be computed as described in the theoretical section of this paper. The following sections will describe the network analyzer used in the measurement technique, the design and construction of the open-ended coaxial line, and the apparatus constructed to measure the dielectric properties of powders at different densities and as a function of temperature.

COAXIAL LINE

Currently, there are open-ended coaxial probes available that are made specifically for dielectric-property measurements. Unfortunately, the work reported here was initiated before these probes were available. Since the need for a probe or rigid coaxial line evolved in order to accomplish the tasks of dielectric-property measurements, the USBM developed and constructed its own coaxial line. The probe concept is the same as those presently available; however, the USBM coaxial line functions at elevated temperatures. The air-filled coaxial line was constructed of type 304 stainless steel and was fitted with a 7-mm, automatic-phase-control flange so that it could be easily connected to the network analyzer. The stainless steel was chosen for its high electrical conductivity and its low thermal conductivity, since measurements were to be performed at elevated temperatures. A stainless steel line also ensured a rigid coaxial cable to enable the measurement of solid samples. The length of the line was 30 cm and the capability to cool the line with water jackets was incorporated. Since the maximum operational temperature of the network analyzer was 50 °C, ensuring a stable temperature at the network analyzer and coaxial line interface was very important.

The termination port on the network analyzer had an impedance of 50 Ω. Thus, for matching purposes, the coaxial line was designed and constructed to maintain the 50-Ω impedance using the following equation (*15*):

$$Z_o = \frac{60 \ln\left(\frac{b}{a}\right)}{\sqrt{\varepsilon_r'}}, \qquad (16)$$

where ε_r' = dielectric constant of the material that fills the coaxial line.

To maintain an impedance of 50 Ω, it was necessary for the ratio of the outer conductor radius to the inner conductor radius to be 2.3 for an air-filled line. It was necessary to insert a thin spacer at the end of the coaxial line. The purpose of the spacer was twofold: (1) it held the center conductor in place, and (2) it excluded materials from the space between the conductors during the measurements. However, the selection of the spacer material was very important. The material had to have very low dielectric properties throughout the frequency range of interest, $\varepsilon_r' < 3$ and $\varepsilon_r'' < 0.0004$, and it had to maintain its structure and composition at the elevated temperatures. The material chosen was a Vespel polymer with very low dielectric properties similar to that of Teflon polytetrafluoroethylene but with a higher melting temperature, ~ 500 °C in an inert atmosphere. To compensate for the Vespel polymer spacer at the end of the line, the conductor ratio in equation 16 was adjusted to maintain the 50-Ω impedance. Using 2.1 for the dielectric constant of Vespel polymer, the radius ratio became 3.54. Thus, the radius of the inner conductor was reduced by an amount to maintain this ratio, but only for the end of the line where the spacer was positioned as shown in figure 3. Figure 4 is a photograph of the coaxial line constructed for this measurement method.

The coaxial line was also designed so impedance standards for calibration of the network analyzer, such as a short circuit and a 50-Ω matching load, could be secured at its end. Calibrating the network analyzer at the end of the coaxial line permitted measurements of the reflection coefficients to be taken at the coaxial cable and mineral interface. This feature eliminated the necessity of dealing with signal delays that are inherent in a system when adding an electrical device of a given length away from the calibration port of the measurement equipment. The same impedance standards included with the measurement equipment were used for the calibration at the end of the coaxial cable. However, the manufacturer's fittings were replaced with ones made specifically to fit at the end of the coaxial line. Also, it should be noted that a shielded open circuit was not used in these calibrations. Figure 5 is a photograph of the impedance standards constructed for calibration of the test equipment.

Figure 3

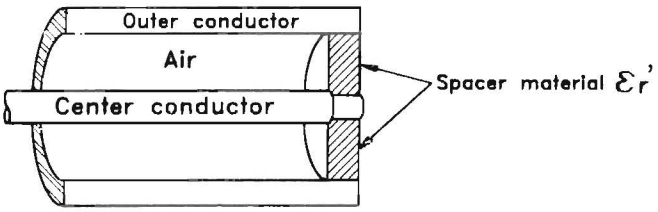

End of the coaxial line where the spacer was placed.

Figure 4

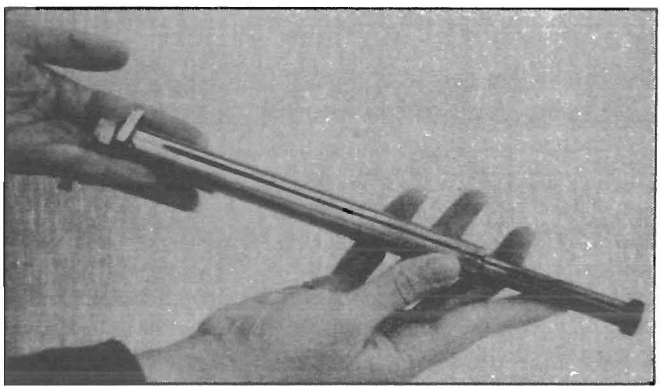

Coaxial line constructed for this measurement method.

Figure 5

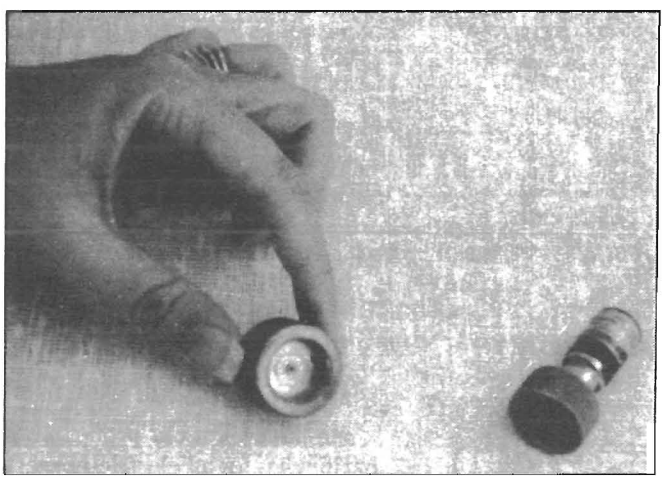

Impedance standards constructed for calibration of test equipment.

NETWORK ANALYZER

The reflection coefficients were measured with an HP8753A network analyzer in conjunction with an HP85044A transmission-reflection test set. The network analyzer supplied a signal to the end of the coaxial line through the transmission-reflection test set and measured the magnitude and phase of the applied and reflected voltage by means of a high-resolution synthesized signal source and a dual-channel, three-input receiver. Comparison of these voltages gave the complex reflection coefficient at the end of the coaxial line. The reflection coefficient could be displayed as real and imaginary parts or as magnitude and phase in rectangular or polar/Smith chart formats. In addition, a microprocessor within the network analyzer could compute the impedance at the end of the coaxial line. The accuracy of the network analyzer was determined by the manufacturer to be within ±1 pct. Figure 6 is a photograph of the network analyzer with the Smith chart display showing the reflection coefficient of a typical high-loss mineral that behaves like a semiconductor.

The network analyzer was controlled by a microcomputer that was programmed to transmit the control signals necessary to sweep the analyzer frequency and record the reflection coefficient data at each frequency step. Data from the analyzer were transmitted to the computer where they were analyzed to determine the dielectric properties of the material at the end of the coaxial line. The network analyzer could also average numerous measurements at each given frequency throughout the sweep and then transmit an averaged value of both the real and imaginary parts measured. For the purposes of these experiments, the value of each reflection coefficient was measured 32 times and averaged.

Figure 6

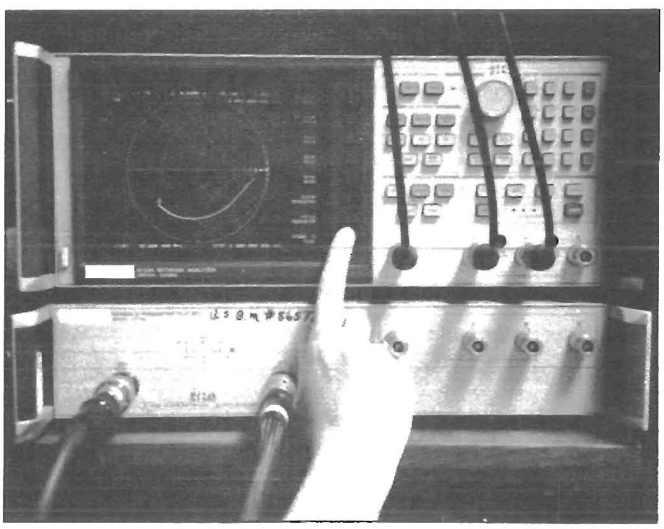

Network analyzer in Smith chart display mode.

HEATING DEVICE

The heating device consisted of two, small, semicircular heaters (figure 7) 7.5 cm in height that, when placed together, left a 5-cm opening in the center. Also, an "internal heater" was placed directly above the sample to provide additional heat, since in some cases the external heaters were not sufficient to bring these minerals to the desired higher temperature. The opening provided enough space for the mineral sample and the coaxial line. The coaxial line was mounted on a stand that also supported the heaters. An insulating box, pictured in figure 8, housed the heaters and coaxial line and was sealed to maintain an inert atmosphere around the sample during the heating period. A positive pressure of argon gas was maintained in the box to eliminate oxidation of the sample while it was heated. A Type-K thermocouple was positioned along the side of the coaxial line to measure the surface temperature of the material during the heating and measurement cycle.

DENSITY CHAMBER

In order to vary the densities of the powdered mineral samples and to measure the dielectric properties of the minerals at various densities, a variable density chamber was designed and constructed. It was necessary for this apparatus to provide an easily measurable change in the mixture density without changing the sample weight inside. A cylindrical chamber was constructed of a very low-loss material to ensure that none of the transmitted signal was reflected from the apparatus, which would interfere with the dielectric property measurements. The density measurements were accomplished by placing a predetermined amount of the powdered mineral into the chamber of

Figure 7

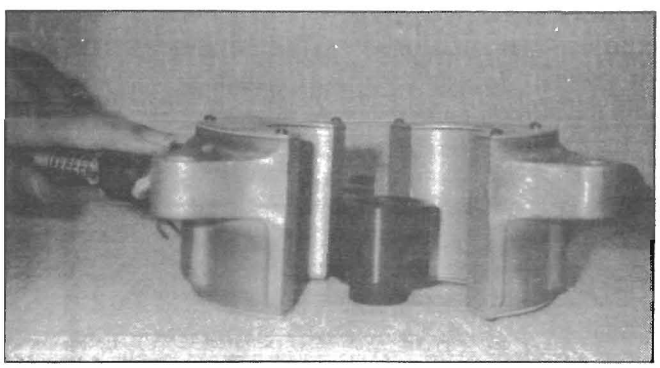

Heaters used in the measurement system to heat mineral samples to temperatures of 325 °C.

known volume. The floor of the chamber was actually a piston that provided a volume change inside the density chamber. The open end of the coaxial line was fitted with a grounding plane and was secured on the top of the density chamber. Once the chamber was filled with a mineral sample, the piston was moved in a vertical direction until the sample was seated against the coaxial line. The Smith chart display on the network analyzer indicated when the coaxial line and the mineral were in electrical contact. The movement of the piston floor was calibrated to determine the volume change inside the chamber. By knowing the weight and volume of the sample, the density of the powder-air mixture was calculated. Figure 9 is a drawing that depicts the apparatus including the coaxial line, heating device, and density chamber. Figure 10 is a photograph of the density apparatus, and figure 11 is a photograph of the complete measurement system.

Figure 8

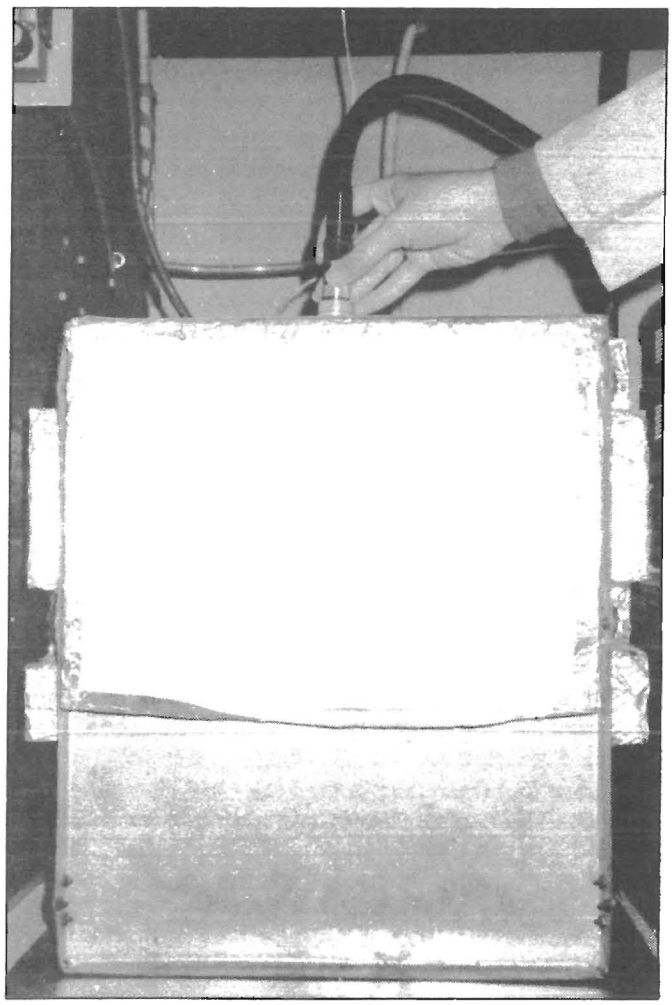

Insulating box used to house the heating apparatus and mineral samples to alleviate sample oxidation during the heating cycle.

Figure 9

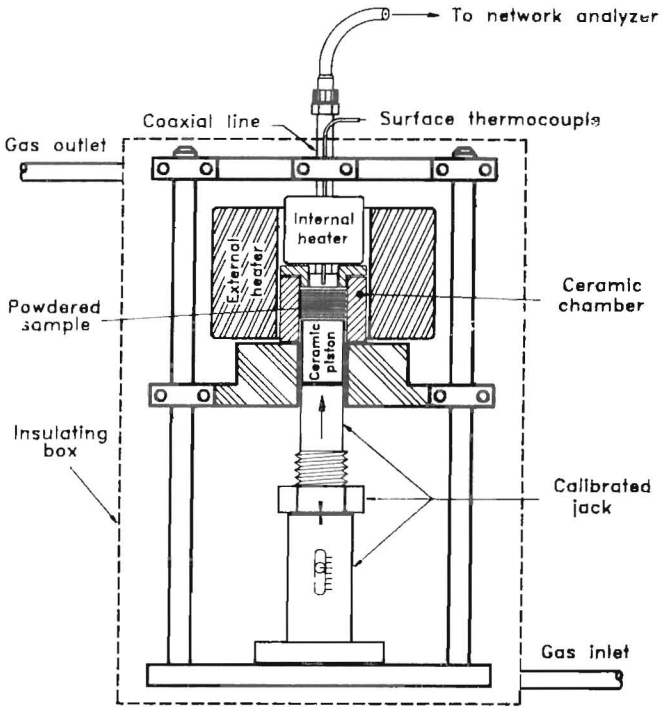

Holding apparatus constructed for measuring dielectric properties of minerals as a function of temperature and density.

Figure 10

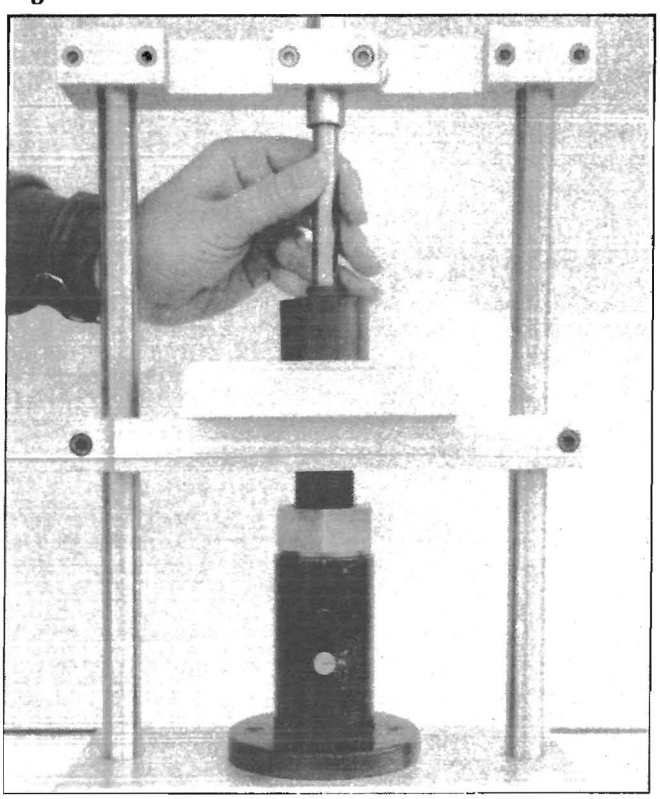

Density variation apparatus.

Figure 11

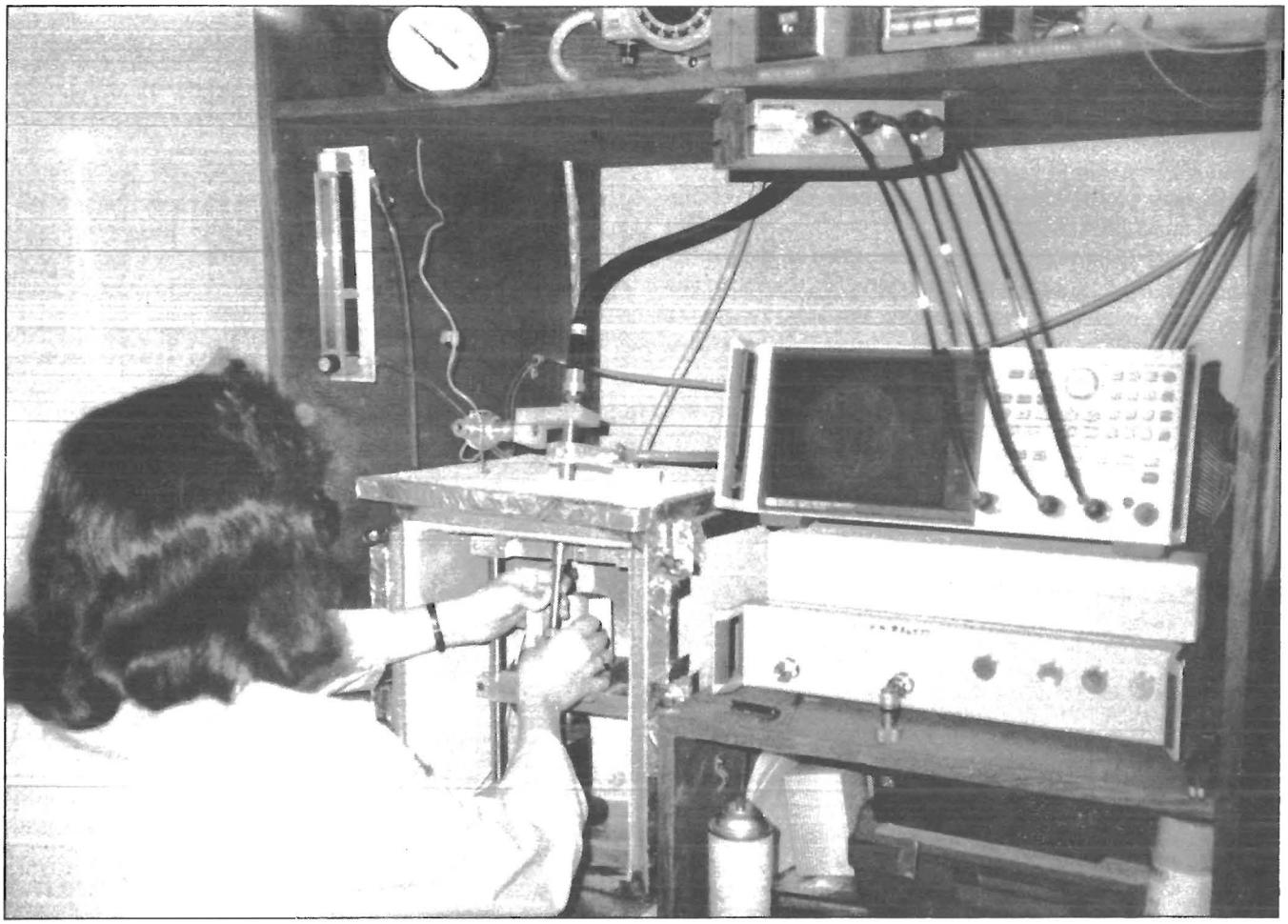

Complete measurement system.

EXPERIMENTAL PROCEDURE

The procedure used to determine the dielectric properties of minerals as a function of temperature, density, and frequency included preparing the minerals for measurement, calibration of the network analyzer, sample measurement, and data evaluation. The following sections give a detailed description of each step in the measurement process.

SAMPLE PREPARATION

The minerals selected for measurement were obtained from various sources such as chemical supply companies, mineral supply companies, and mines. These minerals were not pure specimens, but were often found in conjunction with other substances such as quartz. In order to obtain accurate data on the dielectric properties of the mineral, this gangue had to be separated from the mineral. Various methods were used to accomplish this including the use of Dicer separating tables, which separated the materials by density differences. These purified minerals were then crushed to fine powders (<40 μm) to facilitate the measurement of their dielectric properties as a function of density. X-ray analysis was performed on each mineral tested to identify the impurities, if any, and this information was documented. The particle density of the purified minerals was ascertained by use of a helium pycnometer, and these results were later used to calculate the dielectric properties of each mineral at its solid density.

CALIBRATION OF NETWORK ANALYZER

Before the dielectric properties of a mineral could be measured, the network analyzer had to be calibrated. The calibration of the system and the measurements were performed at the coaxial line and mineral interface unlike all other open-ended coaxial systems where calibrations are

performed at the other end of the coaxial line. The procedure included setting the upper and lower limits of the swept frequencies to include only those of interest, and then calibrating with an open circuit, a short circuit, and a 50-Ω matching load. The calibration was checked by reattaching the impedance standards and, if within acceptable limits, stored in the memory of the network analyzer. To test whether the calibration would be affected by heating the coaxial line, the impedance standards were attached to the line and heated to 325 °C. This test indicated that the calibration was stable over the entire temperature range. When the calibration of the network analyzer was completed, the measurement of the dielectric properties of the minerals could begin.

DIELECTRIC PROPERTY MEASUREMENTS

The entire powdered mineral sample was weighed, a portion was poured into the density chamber, and the remainder was weighed again. The difference was the mass of mineral measured, and this value was entered in the record. An infinite shorting plane was attached to the coaxial line and then positioned on top of the density chamber. The piston was turned to decrease the volume inside the density chamber until the Smith chart showed that the coaxial line was in contact with the mineral sample. At this point, the volume inside the chamber was recorded and the density of the powder-air mixture was determined from the mass of mineral and the volume occupied by the mineral inside the chamber. The insulating box was then closed and flushed for 20 min with argon gas to remove as much air as possible from the box so the mineral would not oxidize while it was being heated. While the system was being purged with the inert gas, the dielectric properties of the mineral were measured at room temperature. This was done through initiation of a computer program written specifically for the purpose of remotely controlling the transport of data in the proper format from the network analyzer to a disk in the computer. The data were stored on the disk for future evaluation. The measurement of the dielectric properties of the minerals at different temperatures was begun after the insulating box was purged. As described earlier, the coaxial line was equipped with a Type-K thermocouple mounted down the length of the line that enabled temperature measurements at the surface of the mineral sample. Earlier experiments had shown there was no need to ensure a small temperature gradient within the material since the signal from the network analyzer only penetrated the surface of the sample, given the small depth of penetration inherent with high-loss materials. The thermocouple was connected to a programmable, digital temperature controller that monitored the heater outputs to control sample heating rates. The dielectric properties of the minerals were measured and saved on disk at 75, 100, 125, 175, 200, 225, 275, 300, and 325 °C. This process was repeated until the dielectric properties of the minerals were obtained over the entire temperature range for at least three different densities.

Following the collection of the dielectric property data, the data were evaluated. To begin with, the values of the fringing capacitances had to be determined. The dielectric properties of saline solutions of known normalities were measured at room temperature and used to determine the fringing capacitances by the method previously described. The values of the fringing capacitances were inserted into computer programs written to calculate the dielectric properties of the mineral at each temperature and density. These data were stored on disks and later used in computer programs written to calculate the dielectric properties of the mineral at its theoretical density at each temperature. The calculated dielectric properties of the mineral at its theoretical density were plotted as functions of frequency and temperature to demonstrate how the dielectric properties were affected by the different variables. Some of these plots are included in the following section.

RESULTS

The dielectric properties of more than 60 minerals have been measured by this technique. For every mineral measured, the measurement frequency was swept from 300 MHz to 3 GHz in 27-MHz intervals. Each mineral was measured at a minimum of three different densities and, at each density, dielectric-property data were taken at temperatures of 25, 75, 100, 125, 175, 200, 225, 275, 300, and 325 °C. The dielectric properties of the minerals change with increasing temperature, indicating that the material's absorption to microwave energy change as they were heated. As an example of typical dielectric-property data, figures 12 and 13 display the measured data in graphic form for the mineral chalcopyrite, CuFeS, in the frequency range of 300 MHz to 3 GHz. The data are shown for temperatures of 25, 100, 200, and 300 °C. The trends observed in the dielectric properties for chalcopyrite were similar to those observed in most of the minerals measured.

Two minerals that did not display similar trends were chalcocite, Cu_2S, and cobaltite, CoAsS. Figures 14 and 15 are graphs of the dielectric constant and loss factor, respectively, of chalcocite as a function of frequency in the

temperature range of 25 to 300 °C. The dielectric constant and loss factor of chalcocite increased as expected until the mineral reached 100 °C, when they started to decrease. After investigating, it was found that Cu_2S experienced a phase change at about 100 °C, where its crystalline structure changed from orthorombic to isometric (*16*). Figures 16 and 17 depict the dielectric constant and loss factor, respectively, of chalcocite as a function of temperature for the two distinct frequencies of 915 MHz and 2.45 GHz. These graphs illustrate this phenomenon more clearly. None of the other minerals evaluated displayed similar characteristics; however, crystalline phase changes of the other minerals occur at temperatures much higher than 325 °C. Similar changes would be expected in some of the other minerals at higher temperatures.

Figures 18 and 19 are graphs of the dielectric constant and loss factor of cobaltite as a function of frequency at 33, 100, 200, 300, and 325 °C. Again the dielectric constant and loss tangent are frequency and temperature dependent; however, in this case there was an anomaly at 450 MHz. The drastic decrease in the dielectric constant and sudden increase in the loss tangent are probably caused by a resonance of the material that appears to exist at this frequency.

Figures 20 and 21 illustrate the method used for extrapolating the dielectric properties of the mineral to its theoretical, or natural, density given information at other densities. The mineral chosen was chalcopyrite. The values of the dielectric constant and loss factor were calculated from the measured data at four densities, 1.18, 1.31, 1.70, and 2.41 g/cm³. Then, equations 15 and 17 were used to determine the values of ε_r' and ε_r'' at the natural density of chalcopyrite, 4.10 g/cm³. Figure 20 is the plot of the dielectric constant at 915 MHz as a function of density, and figure 21 is a similar plot for the loss factor at 915 MHz. The R^2 (coefficient of determination) values for the curves in figures 20 and 21 are 0.98 and 0.89, respectively.

Figure 12

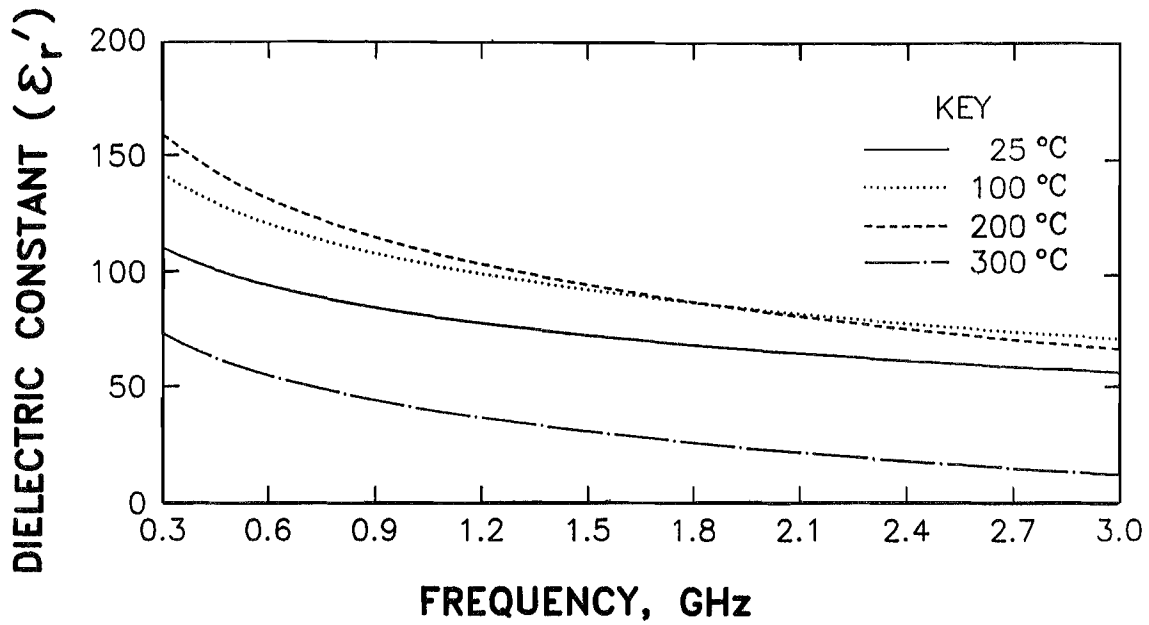

Dielectric constant of chalcopyrite at different frequencies and temperatures.

Figure 13

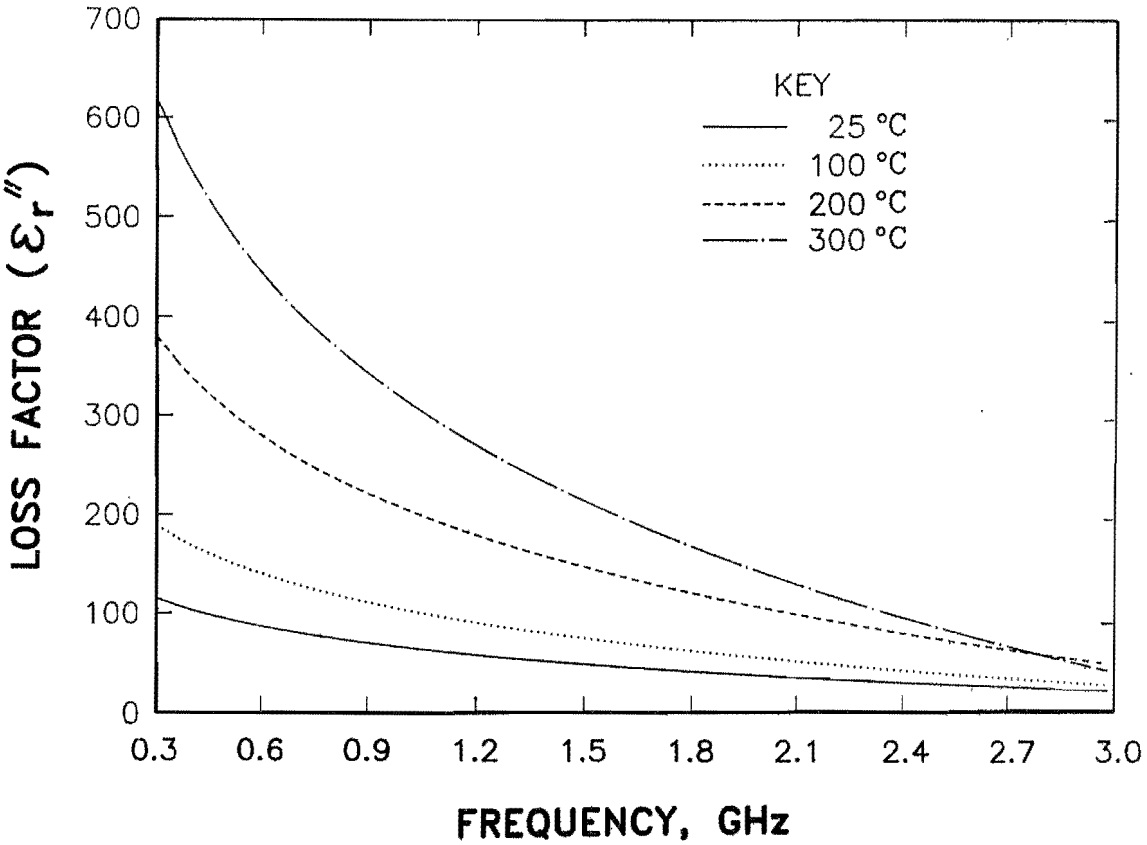

Loss factor of chalcopyrite at different frequencies and temperatures.

Figure 14

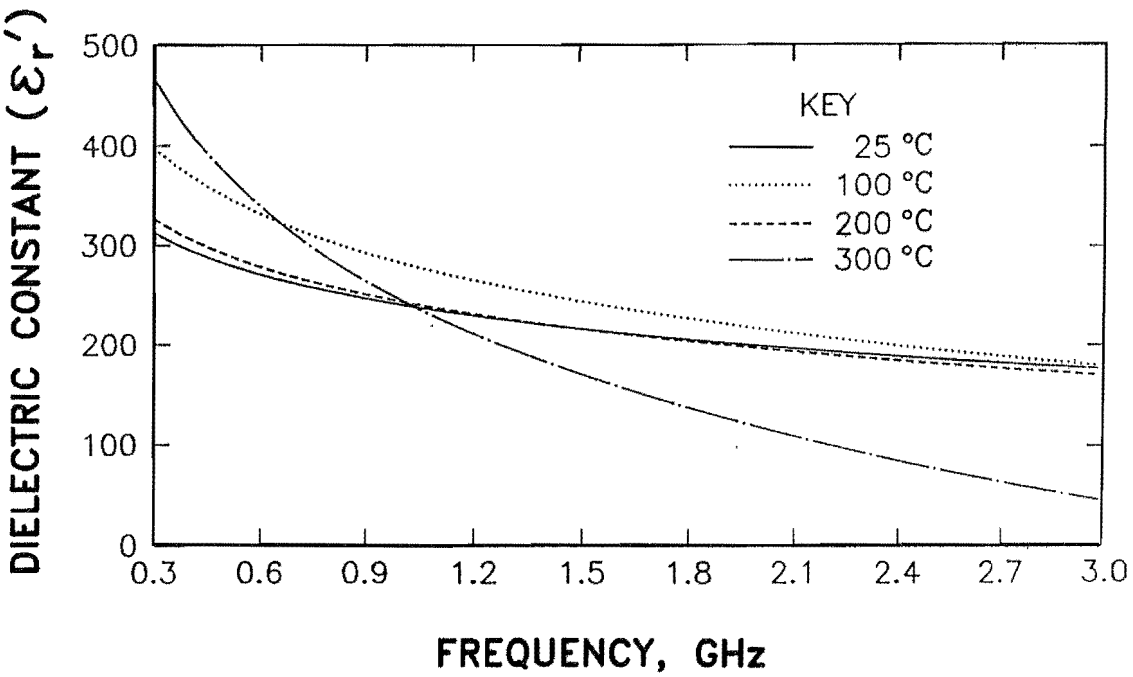

Dielectric constant of chalcocite at different frequencies and temperatures.

Figure 15

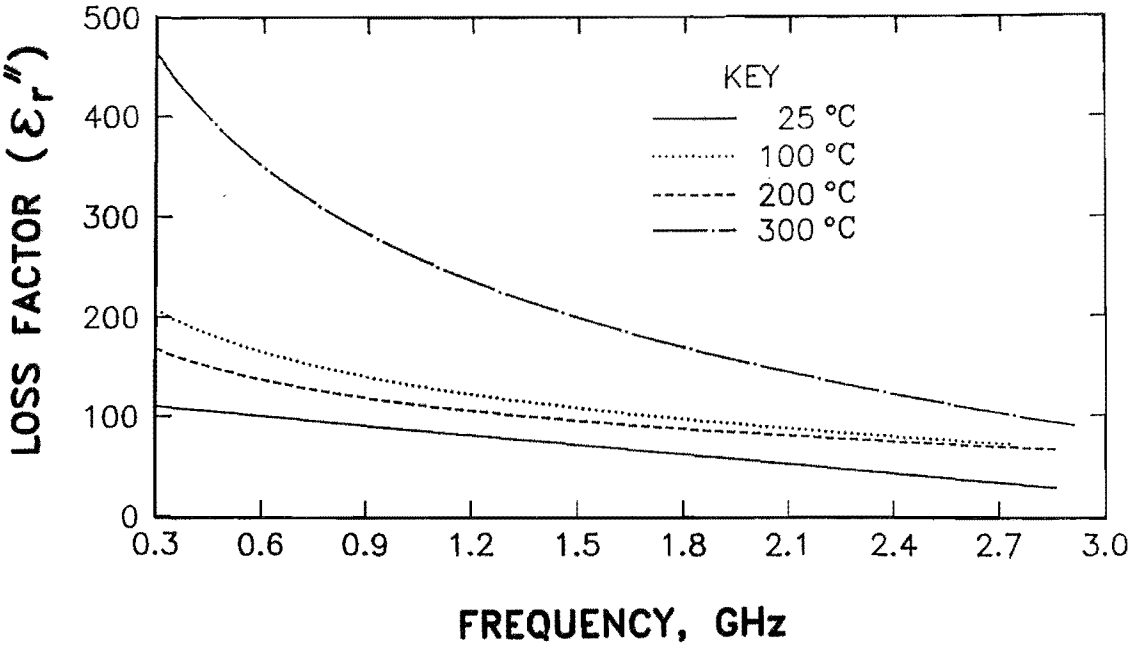

Loss factor of chalcocite at different frequencies and temperatures.

Figure 16

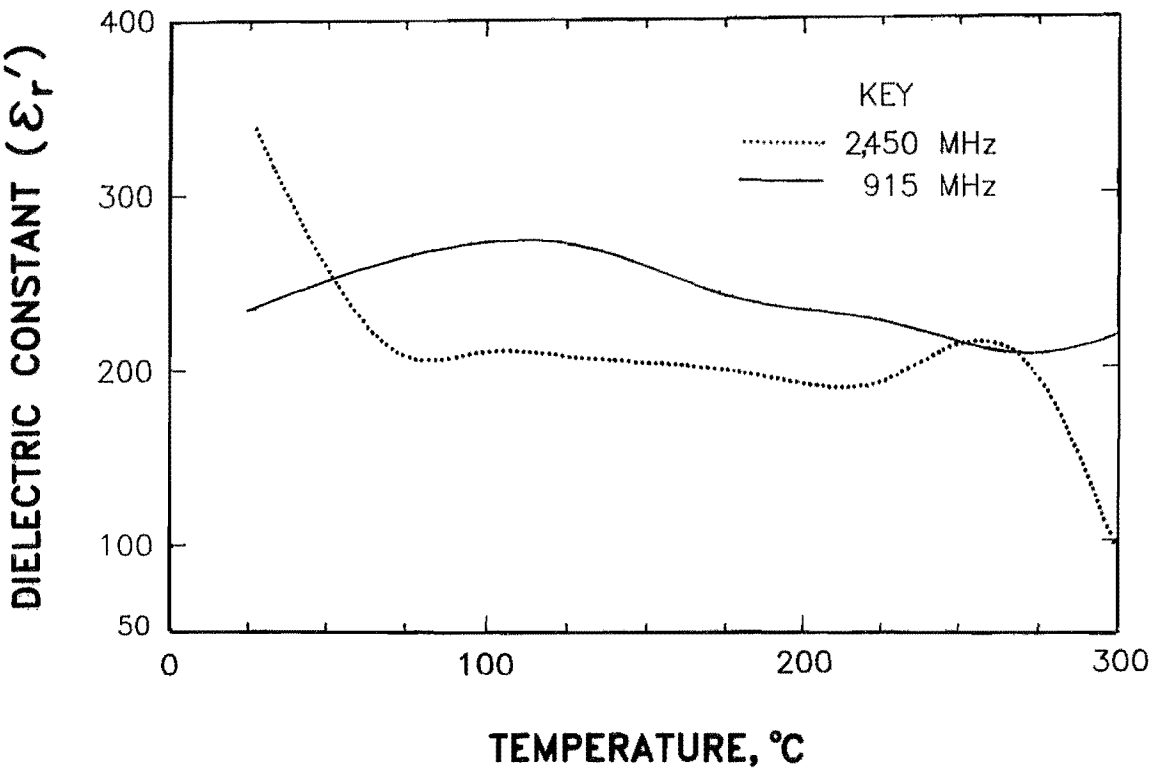

Dielectric constant of chalcocite at different temperatures for two discrete frequencies.

Figure 17

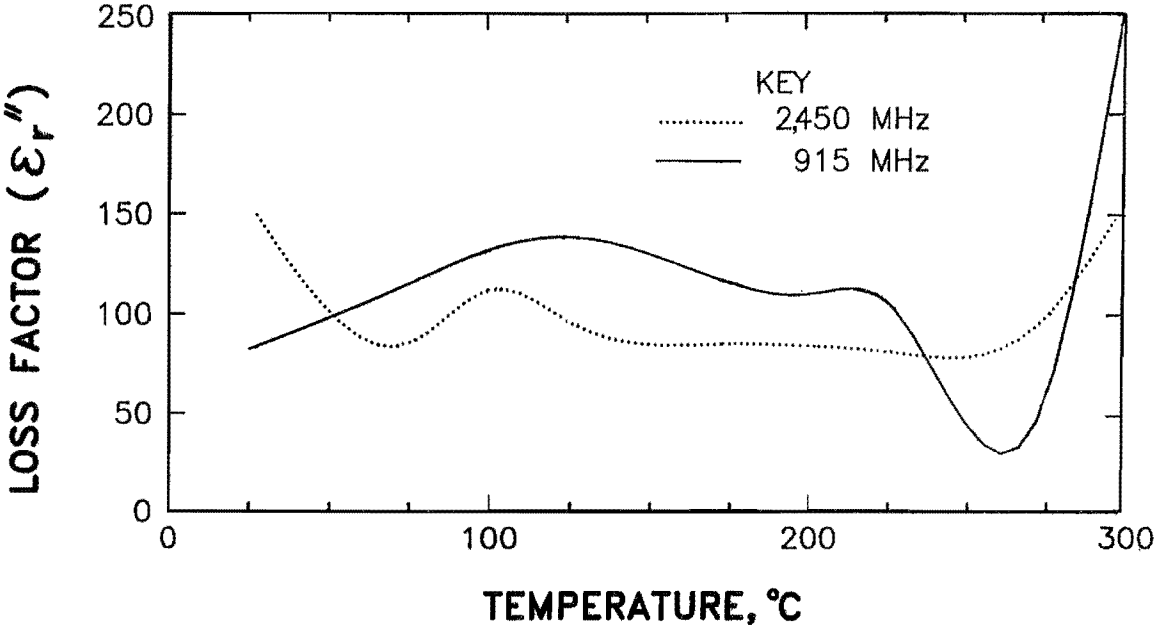

Loss factor of chalcocite at different temperatures for two discrete frequencies.

Figure 18

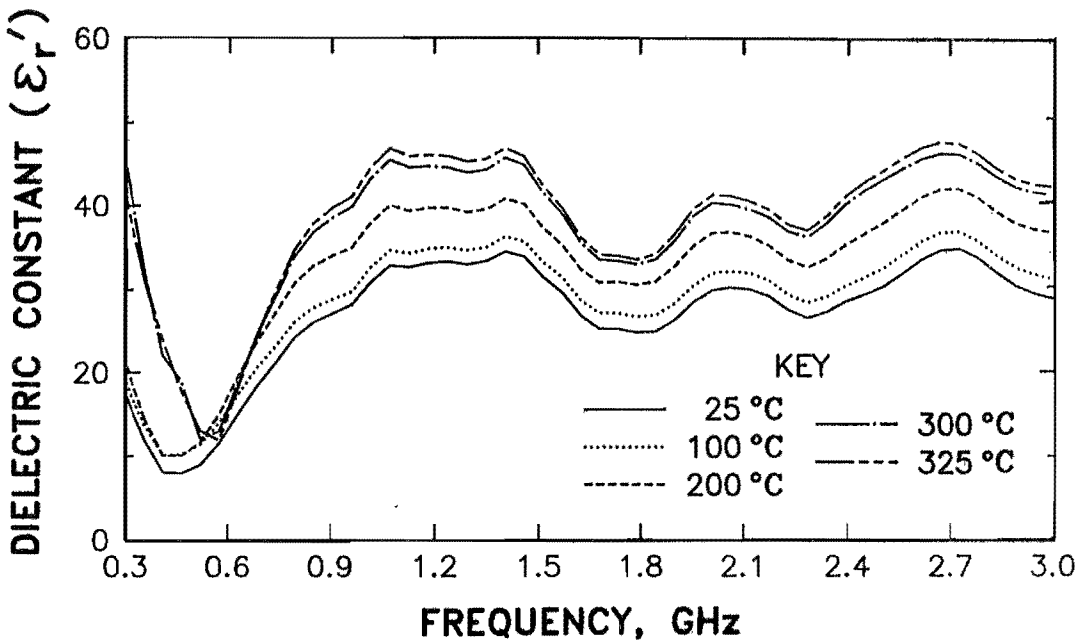

Dielectric constant of cobaltite at different temperatures and frequencies.

Figure 19

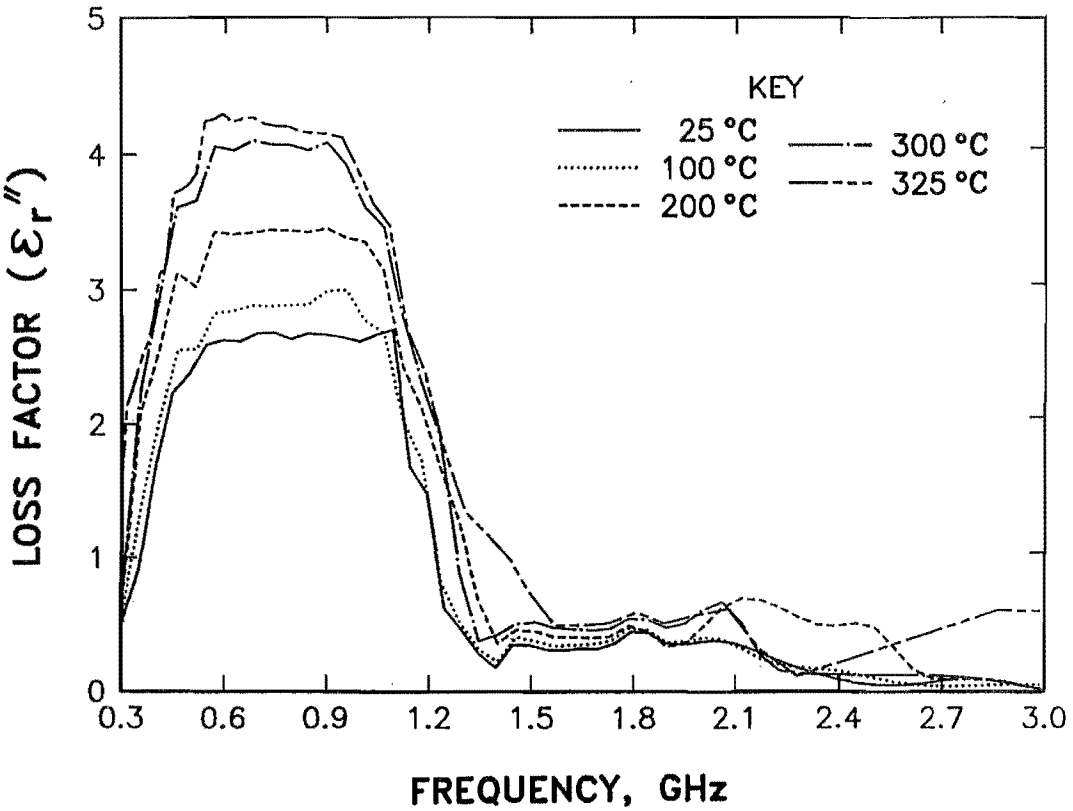

Loss factor of cobaltite at different temperatures and frequencies.

Figure 20

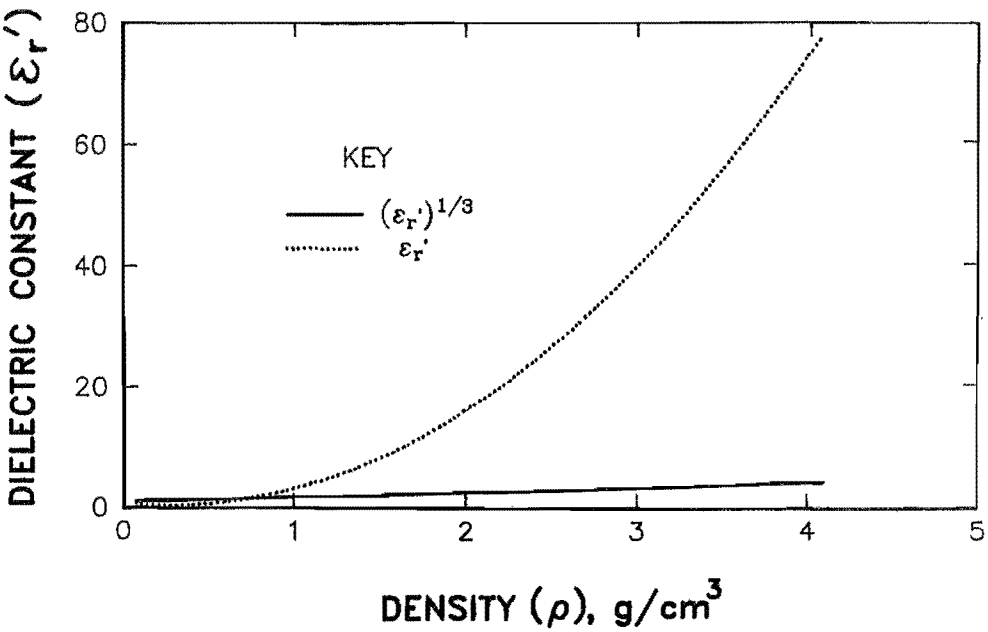

Dielectric constant of chalcopyrite where the dotted line represents a second order polynomial fit of ε_r' versus ρ and the solid line is a representation of a linear regression of $(\varepsilon_r')^{1/3}$ versus ρ.

Figure 21

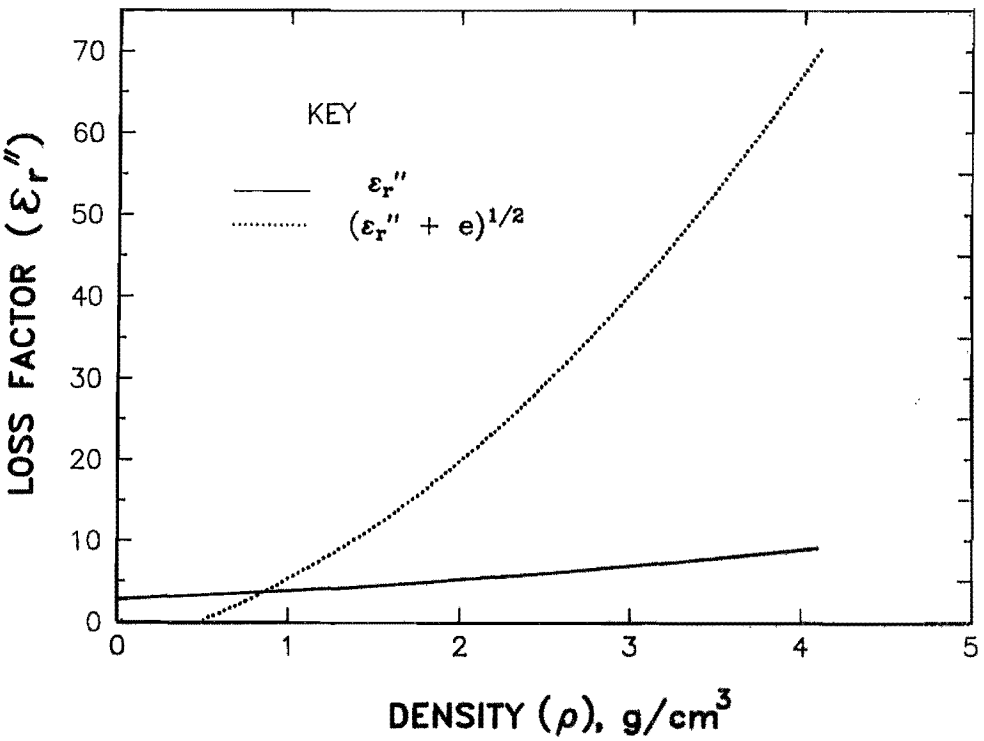

Loss factor of chalcopyrite where the dotted line represents the second order polynomial fit for ε_r'' versus ρ and the solid line is the representation of the linear regression of $(\varepsilon_r'' + e)^{1/2}$ versus ρ.

CONCLUSIONS

The USBM Tuscaloosa Research Center has developed a technique for measuring the dielectric properties of minerals at microwave heating frequencies. This technique was designed to measure the dielectric properties as a function of density in the temperature range of 25 to 325 °C. The measurement system is completely computer controlled and will measure the dielectric properties of liquids, solids, and powders with loss tangents ≥0.01. To date, the USBM has measured the dielectric properties of more than 60 medium- to high-loss minerals and will continue to provide basic data on the dielectric properties of materials at microwave heating frequencies. These basic data will begin to fill the gap that exists in the literature on the dielectric properties of minerals and will aid researchers in evaluating new and improved minerals- and materials-processing techniques using microwave energy.

REFERENCES

1. Parkhomenko, E. I. Electrical Properties of Rocks. Plenum, 1967, 314 pp.

2. Young, K. F., and H. P. R. Frederikse. Compilation of the Static Dielectric Constant of Inorganic Solids. J. Phys. Chem. Ref. Data, v. 2, No. 2, 1973, pp. 313-410.

3. Von Hipple, A. R. (ed.). Dielectric Materials and Applications. MIT Press, 1966, 425 pp.

4. Morgan, S. O., D. Edelson, W. McMahan, and W. J. Merz. Properties of Dielectrics. Ch. in American Institute of Physics Handbook, ed. by D. E. Gray. McGraw-Hill, 5th ed., 1957, pp. 5-114 to 5-117.

5. Nippon Steel Corp. Hot Pressing of Inorganic Materials. Jpn. Pat. Doc. 74/100, 727, Sept. 2, 1974.

6. Meek, T. T. Sintering of a Refractory in a Microwave Field. Paper in UNITECR '89, Am. Ceram. Soc., 1989, pp. 1411-1416.

7. Katz, J. D., R. D. Blake, and C. P. Scherer. Microwave Sintering of Titanium Diboride. Presented at the 13th Annual Conference on Composites and Advanced Ceramics (Cocoa Beach, FL, Jan. 15-18, 1989). Office of Scientific and Technical Information, Dep. Energy, LA-UR-89-533.

8. Hayt, W. H., Jr. Engineering Electromagnetics. McGraw-Hill, 1958, p. 433.

9. Athey, T. W., M. A. Stuchly, and S. S. Stuchly. Measurement of Radio Frequency Permittivity of Biological Tissues with an Open-Ended Coaxial Line: Part I. IEEE Trans. Microwave Theory Tech., v. MTT-30, No. 1, 1982, pp. 82-86.

10. Stuchly, M. A., T. W. Athey, G. M. Samaras, and G. E. Taylor. Measurement of Radio Frequency Permittivity of Biological Tissues with and Open-Ended Coaxial Line: Part II - Experimental Results. IEEE Trans. Microwave Theory Tech., v. MTT-30, No. 1, 1982, pp. 87-91.

11. Stogryn, A. Equations for Calculating the Dielectric Constant of Saline Water. IEEE Trans. Microwave Theory Tech., v. MTT-19, No. 84, 1971, pp. 733-736.

12. Church, R. H., W. E. Webb, and J. B. Salsman. Dielectric Properties of Low-Loss Minerals. USBM RI 9194, 1988, 23 pp.

13. Nelson, S. O. Observations on the Density Dependence of Dielectric Properties of Particulate Materials. J. Microwave Power, v. 18, No. 2, 1983, pp. 143-152.

14. Kent, M. Complex Permittivity of Fish Meal: A General Discussion of Temperature, Density and Moisture Content. J. Microwave Power, v. 12, No. 4, 1977, pp. 341-345.

15. Brown, R. G., R. A. Sharpe, W. L. Hughes, and R. E. Post. Lines, Waves, and Antennas - The Transmission of Electric Energy. Wiley & Sons, 1973, p. 259.

16. Dana, E. S. Dana's Manual of Mineralogy. Wiley & Sons, 1944, p. 151.

APPENDIX.—ABBREVIATIONS AND SYMBOLS USED IN THIS REPORT

A	fringing field constant
a	radius of coaxial inner conductor
b	radius of coaxial outer conductor
c	density constant for determination of dielectric constant
C_f	fringing capacitance of the line
C_o	fringing capacitance of the line
d	density constant for determination of dielectric constant
e	density constant for determination of loss factor
ε_r^*	complex dielectric constant
ε_r'	dielectric constant
ε_r''	loss factor
f	frequency
Γ	magnitude of the complex input reflection coefficient
Γ^*	complex input reflection coefficient
j	imaginary quantity, $\sqrt{-1}$
k	density constant for determination of loss factor
ℓ	density constant for determination of loss factor
m	slope of the line in the density equation
N	normality
ω	angular frequency = $2\pi f$
φ	phase of the complex input reflection coefficient
ρ	density of the air-powder mixture
σ	electrical conductivity at a given frequency
$\tan\delta$	loss tangent
Z_L	load impedance
Z_o	characteristic impedance of the coaxial line
λ	wavelength
$\upsilon_{\varepsilon r}$	wavelength inside a material